Dalton Transactions

Accepted Manuscript

ROYAL SOCIETY OF CHEMISTRY

www.rsc.org/dalton

Dalton Transactions

RSCPublishing

ARTICLE

A Series of Cobalt and Nickel Clusters Based on Thiol-containing Ligands Accompanied by *in situ* Ligand Formation

Cite this: DOI: 10.1039/x0xx00000x

Received 00th January 2012,
Accepted 00th January 2012

DOI: 10.1039/x0xx00000x

www.rsc.org/

Song-De Han, Xiao-Hong Miao, Sui-Jun Liu, and Xian-He Bu*

Eight cobalt and nickel clusters with the formulas of $[Co_4(\mu_4\text{-}O)(MBT)_5(\mu_2\text{-}Piv)]$ (**1**), $[Ni_3(MBT)_2(\mathbf{L1})_2(OCH_3)_2]$ (**2**), $[Ni_4(\mu_3\text{-}S)(\mu_3\text{-}S_2)(MBT)_2(\mathbf{L2})]$ (**3**), $[Ni_4(\mathbf{L3})_4]$ (**4**), $[Ni_6(\mu_4\text{-}S)_3(MBT)_6]\cdot(C_2H_5OH)_2$ (**5**), $H[Co_4(\mu_4\text{-}O)(HMBI)_6]\cdot(NO_3)(TEA)_{0.5}(CH_3OH)_2(H_2O)$ (**6**), $[Ni_2(HMBI)_4]\cdot(CH_3OH)_2$ (**7**), and $[Ni_5(MBI)_2(HMBI)_4(OCH_3)_2]\cdot(CH_3OH)_3(H_2O)_2$ (**8**) (HPiv = Pivalic acid, H**L1** = 2-disulfanylbenzo[*d*]thiazole, H_2**L2** = (*Z*)-2-((2-mercaptophenyl)imino)benzo[*d*]thiazole-3(2*H*)-thiol, H_2**L3** = (*Z*)-2-(benzo[*d*]thiazol-2(3*H*)-ylideneamino)benzenethiol, TEA = triethylamine), have been solvothermally prepared via assembling distinct metal resource and thios-containing ligands 2-mercaptobenzothiazole (HMBT)/2-mercaptobenzimidazole (H_2MBI). Complexes **1** and **6** are tetrahedral cobalt clusters. Complex **2** features linear arrangement of nickel ions. Complexes **3** and **4** are tetranuclear nickel clusters with the butterfly and square shape, respectively. Complex **5** displays a trigonal prism geometry. Complexes **7** and **8** exhibit paddle-wheel and trigonal bipyramid geometry, respectively. The starting ligand HMBT suffers *in situ* ligand transformation in the formation of the nickel clusters and the new generated inorganic ligands (S^{2-} and S_2^{2-}) and organic ligands (H**L1**, H_2**L2** and H_2**L3**) were captured within the metallic cores. Magnetic studies indicate that complexes **1** and **6** show dominating antiferromagnetic couplings and that spin frustration exists in **6**.

Introduction

Polynuclear transition-metal complexes have received considerable attentions because of not only their diversity of intriguing architectures and topologies but also their potential applications as functional materials in the fields of magnetism, electrochemistry and catalysis.[1,2] To date, some inspiring accomplishments have been achieved, breaking the record of the corresponding nuclearity. For example, Ag_{490}, Mo_{368}, Mn_{84}, Fe_{168}, Co_{36}, Ni_{34}, Er_{60}, $La_{76}Ni_{60}$, $Cu_{17}Mn_{28}$, and $Fe_{16}Ln_4$ are among the largest clusters to have been studied.[3] Other clusters, such as Mn_{12}, Mn_{32}, Fe_4, Gd_{48}, $Fe_{12}Ln_4$, $Ni_{32}La_{20}$, $Cu_{36}Ln_{24}$, and $Gd_{36}Ni_{12}$ have also been reported, and some of them present single-molecule magnets (SMMs) behaviour or large magnetocaloric effect (MCE).[4] Although remarkable advances have been made in the practical and theoretical approaches, the rational design and synthesis of such materials is still a challenging task for chemists due to the difficulty in controlling the size and nuclearity at a molecular level.

Among the strategies to this target, judiciously choosing a suitable ligand to construct the desirable product via the self-assembly between metal ions and ligands has been gaining more and more favor.[5] In the process of self-assembly, however, most of the used ligands consist of hard donors (oxygen or nitrogen),[3b-j,4,5] and few contain soft donors (like sulfur donor).[3a,6] Recent investigations have demonstrated that using ligand containing soft donors is favorable to enhance the magnetic exchanges between the metal ions and generate different crystal fields.[7] Furthermore, it has also been substantiated that the thiol is prone to take place *in situ* metal/ligand reaction under given conditions, which might give rise to novel or unexpected products.[6e,8] Paralleling the ligands, the sources of metal ions are mainly from metal salts or oxide in the process of assembly,[9] only a few cases are from precursors.[3c,e,j,4e,10] The potential superiorities of utilizing precursors are not only that they serve as the distinctive source of metal ions but also, most importantly, simultaneously as the unique source of other available bridging/chelating ligands and/or building units which sufficiently offer more variability to fabricate complicated and fantastic topologies with interesting properties. Considering all the aspects above, we turned our attention to the rarely examined ligands 2-mercaptobenzothiazole (HMBT) and 2-mercaptobenzimidazole (H_2MBI), and precursors $[M_2(OH_2)(piv)_4(Hpiv)_4]$ (M = Co, Ni;

HPiv = $HO_2CC(CH_3)_3$; abbreviated as Co_2 and Ni_2 hereinafter), exploring their utilities for the construction of transition-metal clusters. Herein, we report a series of cobalt and nickel clusters based on the above-mentioned thiol-containing ligands, that is, $[Co_4(\mu_4\text{-}O)(MBT)_5(\mu_2\text{-}Piv)]$ (**1**), $[Ni_3(MBT)_2(\mathbf{L1})_2(OCH_3)_2]$ (**2**), $[Ni_4(\mu_3\text{-}S)(\mu_3\text{-}S_2)(MBT)_2(\mathbf{L2})]$ (**3**), $[Ni_4(\mathbf{L3})_4]$ (**4**), $[Ni_6(\mu_4\text{-}S)_3(MBT)_6]\cdot(C_2H_5OH)_2$ (**5**), $H[Co_4(\mu_4\text{-}O)(HMBI)_6]\cdot(NO_3)(TEA)_{0.5}(CH_3OH)_2(H_2O)$ (**6**), $[Ni_2(HMBI)_4]\cdot(CH_3OH)_2$ (**7**), and $[Ni_5(MBI)_2(HMBI)_6(OCH_3)_2]\cdot(CH_3OH)_3(H_2O)_2$ (**8**) (H**L1** = 2-disulfanylbenzo[*d*]thiazole, H_2**L2** = (*Z*)-2-((2-mercaptophenyl)imino)benzo[*d*]thiazole-3(2*H*)-thiol, H_2**L3** = (*Z*)-2-(benzo[*d*]thiazol-2(3*H*)-ylideneamino)benzenethiol, TEA = triethylamine). Interestingly, the starting ligand of HMBT suffers *in situ* ligand reaction in the process of forming complexes of **2**-**5**, and new inorganic ligands (S^{2-} and S_2^{2-}) and organic ligands (H**L1**, H_2**L2** and H_2**L3**) have been generated and captured within the metallic units.

Experimental

Materials and instrumentation

All chemicals were of analytical grade (AR) and used as received. The Co_2 and Ni_2 precursors were prepared according to the method described in the literature.[10a,11] Elemental analyses were performed on a Perkin-Elmer 240C analyzer (Perkin-Elmer, USA). IR spectra were measured on a MAGNA-560 (Nicolet) FT-IR spectrometer with KBr pellets. UV-VIS absorption spectra were measured with a UV-3600 (SHIMADZU) spectrophotometer. Powder X-ray diffraction (PXRD) spectra were recorded on a Bruker D8 FOCUS diffractometer with a Cu-target tube and a graphite monochromator. Simulation of the PXRD spectra were carried out by the single-crystal data and diffraction-crystal module of the Mercury (Hg) program available free of charge *via* the Internet at http://www.iucr.org. The magnetic measurements were performed by using an MPMS XL-7 SQUID magnetometer. Diamagnetic corrections were estimated by using Pascal constants and background corrections by experimental measurement on sample holders. Thermogravimetric (TG) analyses were carried out on a Rigaku standard TG-DTA analyzer with a heating rate of 10°C min^{-1} from ambient temperature to 800 °C under nitrogen gas.

Preparation of complexes $[Co_4(\mu_4\text{-}O)(MBT)_5(\mu_2\text{-}Piv)]$ (1). A mixture of HMBT (0.042 g, 0.25 mmol), Co_2 (0.150 g), TEA (0.1 mL) and CH_3CH_2OH (10 mL) was sealed in a Teflon-lined autoclave (20 mL) and heated to 90°C for 48 h then slowly cooled to 30°C in 24 h. Yield: ca. 40% with respect to HMBT. Elemental analysis (%): Calcd. for $C_{40}H_{29}N_5Co_4S_{10}O_3$ (1184.00): H, 2.47, C, 40.57, N, 5.91. Found: H, 2.60, C, 40.23, N, 5.76. IR (KBr pellets, cm^{-1}): 3431(w), 2956(w), 2898(w), 1943(w), 1780(w), 1686(w), 1587(w), 1531(s), 1482(m), 1453(m), 1420(m), 1372(s), 1314(m), 1281(w), 1241(m), 1161(w), 1101(w), 1086(s), 1031(s), 1018(s), 935(w), 891(w), 848(w), 793(w), 749(s), 723(m), 704(m), 610(w), 536(m).

$[Ni_3(MBT)_2(L1)_2(OCH_3)_2]$ (2). A mixture of HMBT (0.250 g, 1.5 mmol), $Ni(NO_3)_2\cdot6H_2O$ (0.291 g, 1 mmol), TEA (0.15 mL) and CH_3OH (10 mL) was sealed in a Teflon-lined autoclave (20 mL) and heated to 90°C for 48 h then slowly cooled to 30°C in 24 h. Yield: ca. 60% with respect to HMBT. Elemental analysis (%): Calcd. for $C_{30}H_{22}N_4Ni_3S_{10}O_2$ (967.29): H, 2.29, C, 37.25, N, 5.79. Found: H, 2.52, C, 37.56, N, 5.53. IR (KBr pellets, cm^{-1}): 3528(w), 2354(w), 1952(w), 1794(s), 1778(s), 1585(w), 1566(w), 1453(m), 1412(s), 1378(s), 1314(w), 1277(w), 1247(m), 1164(w), 1131(w), 1102(w), 1081(m), 1028(s), 1012(s), 976(w), 933(w), 885(w), 846(w), 757(m), 749(s), 719(m), 702(m), 620(w), 612(w), 576(w).

$[Ni_4(\mu_3\text{-}S)(\mu_3\text{-}S_2)(MBT)_2(L2)]$ (3). A mixture of HMBT (0.167 g, 1 mmol), $NiCl_2\cdot6H_2O$ (0.178 g, 0.75 mmol), TEA (0.060 mL) and CH_3CH_2OH (10 mL) was sealed in a Teflon-lined autoclave (20 mL) and heated to 140°C for 48 h then slowly cooled to 30°C in 24 h. Yield: ca. 5% with respect to HMBT. Elemental analysis (%): Calcd. for $C_{27}H_{16}N_4Ni_4S_{10}$ (951.90): H, 1.69, C, 34.07, N, 5.89. Found: H, 1.43, C, 33.85, N, 5.67. IR (KBr pellets, cm^{-1}): 3427(m), 3063(w), 2922(w), 1938(w), 1775(w), 1637(w), 1566(w), 1496(s), 1453(w), 1405(w), 1376(m), 1282(w), 1249(w), 1188(w), 1158(w), 1084(w), 1027(m), 1011(m), 964(w), 927(w), 876(w), 781(w), 751(m), 742(m), 723(w), 615(w), 596(w).

$[Ni_4(L3)_4]$ (4). A mixture of HMBT (0.250 g, 1.5 mmol), $Ni(NO_3)_2\cdot6H_2O$ (0.291 g, 1 mmol), TEA (0.20 mL) and CH_3CH_2OH (10 mL) was sealed in a Teflon-lined autoclave (20 mL) and heated to 140°C for 48 h then slowly cooled to 30°C in 24 h. Yield: ca. 5% with respect to HMBT. Elemental analysis (%): Calcd. for $C_{52}H_{32}N_8Ni_4S_8$ (1260.18): H, 2.56, C, 49.56, N, 8.89. Found: H, 2.13, C, 49.82, N, 9.15. IR (KBr pellets, cm^{-1}): 3423(w), 3059(w), 1637(w), 1576(w), 1461(s), 1435(s), 1383(w), 1290(w), 1259(m), 1201(w), 1154(w), 1081(w), 1045(w), 946(w), 861(w), 767(w), 745(m), 720(w), 613(w), 558(w).

$[Ni_6(\mu_4\text{-}S)_3(MBT)_6]\cdot(C_2H_5OH)_2$ (5). A mixture of HMBT (0.167 g, 1 mmol), Ni_2 (0.150 g), TEA (0.10 mL) and CH_3CH_2OH (10 mL) was sealed in a Teflon-lined autoclave (20 mL) and heated to 140°C for 48 h then slowly cooled to 30°C in 24 h. Yield: ca. 25% with respect to HMBT. Elemental analysis (%): Calcd. for $C_{46}H_{36}N_6Ni_6S_{15}O_2$ (1537.95): H, 2.36, C, 35.92, N, 5.46. Found: H, 2.18, C, 36.23, N, 5.73. IR (KBr pellets, cm^{-1}): 3441(w), 3054(w), 2970(w), 2747(w), 1944(w), 1781(w), 1637(w), 1584(w), 1564(w), 1450(s), 1382(s), 1314(w), 1274(w), 1246(m), 1155(w), 1081(m), 1049(w), 1027(s), 1011(s), 932(w), 874(w), 851(w), 754(s), 747(s), 720(m), 703(m), 613(w).

$H[Co_4(\mu_4\text{-}O)(HMBI)_6]\cdot(NO_3)(TEA)_{0.5}(CH_3OH)_2(H_2O)$ (6). A mixture of H_2MBI (0.150 g, 1 mmol), $Co(NO_3)_2\cdot6H_2O$ (0.291 g, 1 mmol), TEA (0.12 mL) and CH_3OH (10 mL) was sealed in a Teflon-lined autoclave (20 mL) and heated to 85°C for 48 h then slowly cooled to 30°C in 24 h. Yield: ca. 30% with respect to H_2MBI. Elemental analysis (%): Calcd. for $C_{47}H_{48.5}N_{13.5}S_6Co_4O_7$ (1342.60): H, 3.64, C, 42.05, N, 14.08. Found: H, 4.10, C, 42.57, N, 14.25. IR (KBr pellets, cm^{-1}): 3384(m), 3197(m), 2979(m), 2916(m), 2721(w), 1617(w), 1593(w), 1491(m), 1426(s), 1376(s), 1349(s), 1294(m), 1272(s), 1222(m), 1183(w), 1150(w), 1115(w), 1015(w), 998(m),

928(w), 828(w), 741(m), 663(w), 520(w).

$[Ni_2(HMBI)_4]\cdot(CH_3OH)_2$ (7). A mixture of H_2MBI (0.150 g, 1 mmol), $Ni(NO_3)_2\cdot 6H_2O$ (0.291 g, 1 mmol), TEA (0.10 mL) and CH_3OH (10 mL) was sealed in a Teflon-lined autoclave (20 mL) and heated to 85°C for 48 h then slowly cooled to 30°C in 24 h. Yield: ca. 60% with respect to H_2MBI. Elemental analysis

Table 1. Crystal data and structure refinement parameters for complexes **1**–**8**.

	1	**2**	**3**	**4**
Formula	$C_{40}H_{29}N_5Co_4S_{10}O_3$	$C_{30}H_{22}N_4Ni_3S_{10}O_2$	$C_{27}H_{16}N_4Ni_4S_{10}$	$C_{52}H_{32}N_8Ni_4S_8$
*M*r (g mol^{-1})	1184.00	967.29	951.90	1260.18
Space group	$P2_1/c$	$P\bar{1}$	$P2_1/c$	$P2_1/c$
Crystal system	Monoclinic	Triclinic	Monoclinic	Monoclinic
a (Å)	12.582(3)	7.6972(15)	9.5006(19)	13.969(3)
b (Å)	18.775(4)	9.965(2)	16.608(3)	25.511(5)
c (Å)	21.716(7)	12.372(3)	20.842(4)	15.810(7)
α(°)	90	94.89(3)	90	90
β(°)	116.95(2)	96.17(3)	98.14(3)	120.22(2)
γ(°)	90	110.77(3)	90	90
V (Å^3)	4573(2)	874.4(4)	3255.6(11)	4868(3)
Z	4	1	4	4
F(000)	2384	490	1912	2560
Dc (gcm^{-3})	1.720	1.837	1.942	1.719
μ (mm^{-1})	1.927	2.234	2.949	1.915
R_{int}	0.0479	0.0459	0.1328	0.1634
limiting indices	-16≤ h ≤16 -24≤ k ≤24 -28≤ l ≤28	$-9 \le h \le 9$ $-11 \le k \le 11$ $-14 \le l \le 14$	$-11 \le h \le 11$ $-19 \le k \le 19$ $-24 \le l \le 24$	$-18 \le h \le 18$ $-33 \le k \le 33$ $-20 \le l \le 20$
Collected reflections	47391	7439	26348	47568
Unique reflections	10482	3071	5729	11150
GOF on F^2	1.087	1.062	1.184	1.074
R_1, wR_2 [$I>2\sigma(I)$]	0.0452 0.0810	0.0487 0.1194	0.0983 0.1813	0.0875 0.1106
R_1, wR_2 [all data]	0.0645 0.0871	0.0574 0.1240	0.1356 0.1949	0.1845 0.1329

	5	**6**	**7**	**8**
Formula	$C_{46}H_{36}N_6Ni_6S_{15}O_2$	$C_{47}H_{48.5}N_{13.5}S_6Co_4O_7$	$C_{30}H_{28}N_8Ni_2S_4O_2$	$C_{47}H_{50}N_{12}Ni_5S_6O_7$
*M*r (g mol^{-1})	1537.95	1342.60	778.26	1380.83
Space group	$P2_1/n$	$P2_13$	$P2_1/c$	$R\bar{3}c$
Crystal system	Monoclinic	Cubic	Monoclinic	Trigonal
a (Å)	15.384(3)	18.737(2)	10.426(2)	18.546(3)
b (Å)	15.673(3)	18.737(2)	18.052(4)	18.546(3)
c (Å)	25.018(5)	18.737(2)	19.622(6)	29.647(6)
α(°)	90	90	90	90
β(°)	103.45(3)	90	118.48(2)	90
γ(°)	90	90	90	120
V (Å^3)	5867(2)	6578.3(13)	3246.1(14)	8831(2)
Z	4	4	4	6
F(000)	2904	2436	1600	3816
Dc (gcm^{-3})	1.637	1.359	1.592	1.562
μ (mm^{-1})	2.455	1.223	1.460	1.826
R_{int}	0.1125	0.0821	0.0839	0.0607
limiting indices	$-20 \le h \le 16$ $-20 \le k \le 20$ $-32 \le l \le 32$	$-22 \le h \le 22$ $-22 \le k \le 22$ $-22 \le l \le 22$	$-13 \le h \le 13$ $-23 \le k \le 23$ $-25 \le l \le 25$	$-22 \le h \le 22$ $-22 \le k \le 22$ $-34 \le l \le 34$
Collected reflections	50528	57198	32039	24321
Unique reflections	13854	3866	7383	1734
GOF on F^2	0.908	1.183	1.056	1.220
R_1, wR_2 [$I>2\sigma(I)$] [a]	0.0508 0.1208	0.0562 0.1318	0.0602 0.0902	0.0548 0.1328
R_1, wR_2 [all data] [b]	0.0840 0.1381	0.0617 0.1345	0.1113 0.1029	0.0610 0.1360

[a] $R_1 = \sum ||F_o| - |F_c|| / \sum |F_o|$. [b] $wR_2 = \{\sum[w(F_o^2 - F_c^2)^2] / \sum w(F_o^2)^2\}^{1/2}$.

(%): Calcd. for $C_{30}H_{28}N_8Ni_2S_4O_2$ (778.26): H, 3.63, C, 46.30, N 14.40. Found: H, 3.32, C, 46.58, N, 14.75. IR (KBr pellets, cm^{-1}): 3913(w), 3383(s), 3143(m), 3070(m), 2966(m), 2935(m), 2900(m), 2831(m), 1934(w), 1769(w), 1593(w), 1488(m), 1429(s), 1417(s), 1381(s), 1361(s), 1347(s), 1297(m), 1278(s), 1225(m), 1179(m), 1146(w), 1111(w), 1087(w), 1020(m), 925(w), 844(w), 788(w), 756(m), 746(s), 680(w), 637(w), 582(w), 541(m).

$[Ni_5(MBI)_2(HMBI)_4(OCH_3)_2]\cdot(CH_3OH)_3(H_2O)_2$ (8). A mixture of H_2MBI (0.150 g, 1 mmol), $Ni(NO_3)_2\cdot6H_2O$ (0.291 g, 1 mmol), TEA (0.08 mL) and CH_3OH (10 mL) was sealed in a Teflon-lined autoclave (20 mL) and heated to 120°C for 48 h then slowly cooled to 30°C in 24 h. Yield: ca. 30% with respect to H_2MBI. Elemental analysis (%): Calcd. for $C_{47}H_{50}N_{12}Ni_5S_6O_7$ (1380.83): H, 3.65, C, 40.88, N, 12.17. Found: H, 3.97, C, 40.43, N, 12.58. IR (KBr pellets, cm^{-1}): 3378(m), 3135(m), 3055(m), 2961(m), 2889(m), 2821(m), 2724(m), 2646(m), 1790(s), 1619(m), 1595(m), 1500(w), 1468(w), 1410(s), 1384(s), 1356(s), 1325(m), 1278(m), 1219(m), 1190(m), 1149(m), 1117(w), 1022(m), 933(w), 846(w), 741(s), 682(w), 636(w), 555(w).

Crystallographic data collection and refinement

The single-crystal X-ray diffraction data of complexes **1**-**4**, **6**-**8** were collected on a Rigaku SCX-mini diffractometer at 293(2) K with Mo-Kα radiation (λ = 0.71073 Å) by ω scan mode. The crystallographic data of **5** was collected on a Rigaku MSC diffractometer at 113(2) K with Mo-Kα radiation (λ = 0.71073 Å). The program *CrystalClear* was used for the integration of the diffraction profiles.[12] All structures were solved by direct method using the SHELXS program of the SHELXTL package and refined by full-matrix least-squares methods with SHELXL (semi-empirical absorption corrections were applied by using the SADABS program).[13] Metal atoms in each complex were located from the *E*-maps and other non-hydrogen atoms were located in successive difference Fourier syntheses and refined with anisotropic thermal parameters on F^2. The highly disordered units (solvent molecules and TEA) in complexes **5**, **6**, **8** were treated by the "SQUEEZE" method as implemented in PLATON[14] and the results were appended to the bottom of the CIF file. Detailed crystallographic data are summarized in Tab. 1 and the selected bond lengths and angles are given in Tab. S2. Full crystallographic data for **1**-**8** have been deposited with the CCDC (1013607-1013614). These data can be obtained free of charge from The Cambridge Crystallographic Data Centre via www.ccdc.cam.ac.uk/data_request/cif.

Results and discussion

Syntheses

The different coordination modes of M^{II} (M = Co, Ni) ions and reacting temperature play an important role in the construction of the final clusters. Analyzing the structures of the resulting clusters, we could see that the Co^{II} ions adopts tetrahedral coordination modes in the creation of the clusters, while the Ni^{II} ions feature both tetrahedral and square coordination modes, particular the square coordination mode in the clusters containing *in situ* generated ligands. It is notable that HMBT undergoes *in situ* ligand conversion when reacting with nickel salt and Ni_2 precursor. The nickel resources and reacting temperature are main factors in affecting the *in situ* reaction of HMBT. Reacting HMBT with $Ni(NO_3)_2\cdot6H_2O$ at 90°C, H**L1** was generated and captured within complex **2**. Assembling HMBT and distinct nickel resources ($NiCl_2\cdot6H_2O$, $Ni(NO_3)_2\cdot6H_2O$, Ni_2 precursor) at 140°C, H**L2**, H**L3**, H**L4** were formed and captured within complexes **3**-**5**, respectively. Replacing HMBT with the similar ligand H_2MBI and finely tuning the molar ratio between reactants and reacting temperature, complexes **6**-**8** were prepared. The *in situ* ligand conversion of HMBT in the formation of the nickel cluster is unexpected and interesting. However, the "black-box" nature of the sealed solvothermal reactor makes it very difficult to truly master the reaction mechanisms or even isolate intermediate phases that appear prior to the onset of the product in most solvothermal reactions. The *in situ* reaction can be divided into two groups: the first is the transformation of organic sulfur (mercapto-group) into inorganic sulfur (S^{2-} and S_2^{2-}); the second is the ligand conversion. Analyzing the final result provides a possible explanation for the formation of the resulting ligands (Scheme 1). The *in situ* reaction may be related to the cleavage of C-S bond of the HMBT and the formation of new S-S bond, S-N bond and C-N bond. The cleavage of C-S bond in the presence of Ni^{2+} catalyst has been documented in references.[15] The possible formation routes of the *in situ* generated ligands have been provided in Scheme. S1. In spite of the fact that more than ten types of hydro(solvo)thermal *in situ* ligand reactions are known,[16] the ligand conversion about H_2**L2** and H_2**L3** has not been reported so far.

Description of crystal structures

Crystallographic studies revealed that complex **1** crystallizes in a monoclinic system with space group $P2_1/c$. The core of **1** can be considered as a slightly distorted tetrahedron cluster built from five MBT^- ligands, one Piv^- ligand and one μ_4-O atom occupying the center of the tetrahedron (Fig. 1a). All Co sites are tetracoordinated and locate the vertexes of the

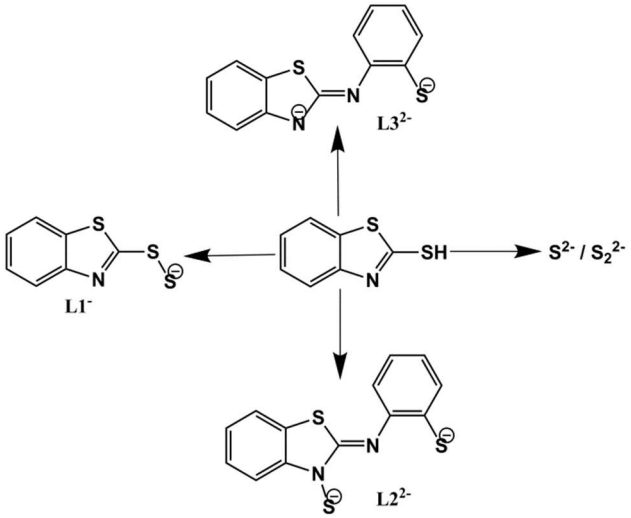

Scheme. 1 The *in situ* reaction of HMBT.

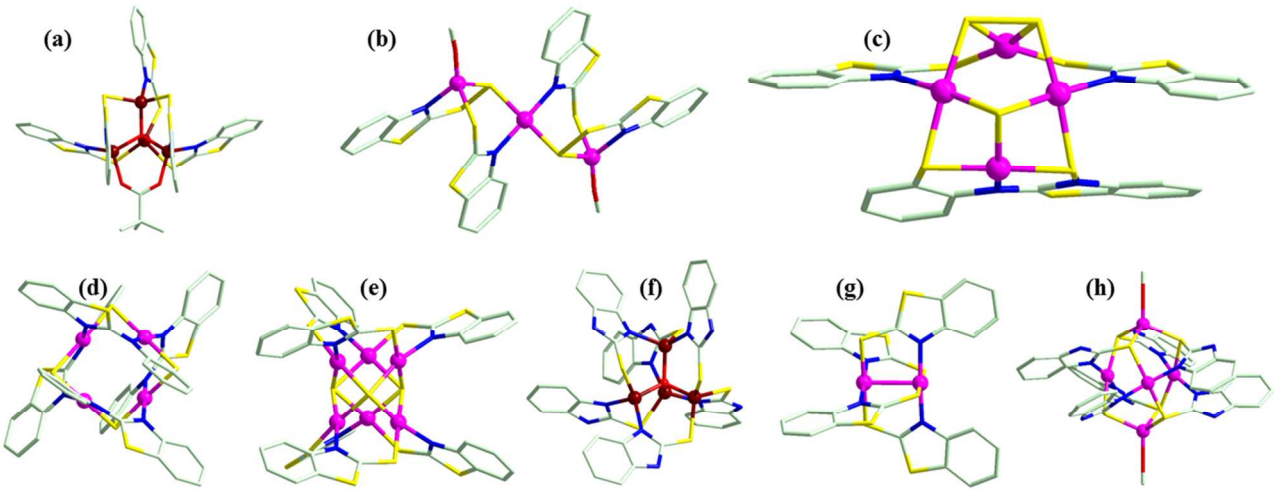

Fig. 1 The structure of complexes **1** (a), **2** (b), **3** (c), **4** (d), **5** (e), **6** (f), **7** (g), **8** (h) (C in light green, O in red, N in blue, S in yellow, Ni in pink, Co in dark red. H atoms and solvent molecules are omitted for clarity).

tetrahedron. All MBT^- ligands offer one N atom and one S atom of mercapto-group to coordinate to Co^{2+} ions. The Co1/Co2 center exhibits a distorted tetrahedral $[CoN_2O_2]$ geometry formed by the coordination of two N atoms from two MBT^- ligands and two oxygen atoms from central μ_4-O atom and carboxylate of Piv^- ligand. The Co3 center shows a distorted tetrahedral $[CoS_3O]$ geometry formed by the coordination of three S atoms from three MBT^- ligands and one O atom from central μ_4-O atom. The distorted tetrahedral coordination sphere of Co4 is $[CoS_2NO]$, in which the S atoms are from two MBT^- ligands, the N atom is from one MBT^- ligand, and the O atom is from the central μ_4-O atom. Neighboring clusters extend into the final 3D supramolecular architecture through intercluster interactions and weak hydrogen bonds of neighboring clusters (Fig. S1†).

Complex **2** crystalizes in a triclinic system with space group *P*-1. The metallic core of **2** could be viewed as a linear trinuclear cluster bridged by two MBT^- ligands and two *in situ* generated $L1^-$ ligands (Fig. 1b). The central Ni1 adopts a square $[CoS_2N_2]$ geometry formed by the coordination of two S atoms from two $L1^-$ ligands and two N atoms from two MBT^- ligands. The terminal Ni2/Ni2A features a tetrahedral $[NiNOS_2]$ geometry formed by the coordination of one N atom from one MBT^- ligand, one O atom from the terminal ligand CH_3O^- and two S atoms from one MBT^- ligand and one $L1^-$ ligand. Adjacent clusters extend into 1D chains *via* π···π stacking (Fig. S2†), which are further connected to 3D supramolecular framework *via* interchain interactions and weak hydrogen bonds of neighboring chains (Fig. S3†).

Complex **3** is a tetranuclear nickel cluster with butterfly-like shape, which could be comprehended as the combination of two triangular Ni_3 clusters sharing the common vertexes. All Ni sites are tetra-coordinated and display a square-planar geometry. The first triangle is linked by one *in situ* generated $\mathbf{L2}^{2-}$ ligand and one $\eta^1{:}\eta^1{:}\eta^1{:}\mu_3\text{-}S^{2-}$ ion. The second triangle is connected by two MBT^- ligands and one $\eta^2{:}\eta^2{:}\mu_3\text{-}S_2^{2-}$ ion (Fig. 1h). The 3D supramolecular architecture was formed through intercluster interactions and weak H-bonds of adjacent clusters (Fig. S4†).

The space group of complex **4** is $P2_1/c$. The metallic core of **4** could be viewed as a square tetranuclear cluster bridged by four *in situ* generated ligands $L3^{2-}$. All Ni sites are tetracoordinated and exhibit a square-planar geometry. All $L3^{2-}$ ligands offer two N atoms and one S atom to coordinate to nickel atoms in $\eta^1{:}\eta^1{:}\eta^2{:}\mu_3$-mode (Fig. 1c). The intercluster interactions and weak H-bonds of neighboring clusters give rise to the final 3D supramolecular architecture (Fig. S5†). Complex **5** possesses a trigonal prism geometry with six nickel ions bridged by twelve MBT^- ligands and three $\eta^1{:}\eta^1{:}\eta^1{:}\eta^1{:}\mu_4\text{-}S^{2-}$ ions (Fig. 1d). All Ni sites feature a square-planar $[NiNS_3]$ geometry formed by the coordination of one N atom from one MBT^- ligand and three S atoms from one MBT^- ligand and two $\mu_4\text{-}S^{2-}$ ions. All MBT^- ligands offer one N atom and one S atom of mercapto-group to coordinate to Ni^{II} ion. The intercluster interactions and weak hydrogen bonds of neighboring clusters lead to the resulting 3D supramolecular architecture (Fig. S6†).

Complex **6** exhibits a tetrahedron geometry with four cobalt ions cobridged by six $HMBI^-$ ligands and one $\mu_4\text{-}O^{2-}$ ion occupying the center of the tetrahedron (Fig. 1e). All Co sites are tetracoordinated. All $HMBI^-$ ligands offer one N atom of imidazole-group and one S atom of mercapto-group to coordinate to cobalt ions. Co1/Co1A/Co1B adopts a tetrahedral $[CoOSN_2]$ geometry formed by the coordination of one O atom from one $\mu_4\text{-}O^{2-}$ ion, one S atom from one $HMBI^-$ ligand and two N atoms from two $HMBI^-$ ligands. Co2 presents a tetrahedral $[CoOS_3]$ geometry accomplished by the coordination of three $HMBI^-$ ligands and one O atom from one $\mu_4\text{-}O^{2-}$ ion. The detailed Bond Valence Sum (BVS) indicates that all cobalt ions are Co^{II} (Tab. S1†), which implies that the tetranuclear cluster is neutral. The negative charge of NO_3^- anion is balanced by the protonated solvent and/or TEA. The presence of NO_3^- anion could also be undisputedly demonstrated by the IR characteristic peaks at about 1349 and 1376 cm^{-1}. Adjacent clusters form a 3D supramolecular architecture by intercluster interactions and weak H-bonds of

neighboring clusters (Fig. S7†).

The structure of complex **7** is the same as the previously reported one with differences only in the solvent molecules.[17] Complex **7** could be envisaged as a paddle-wheel Ni_2 cluster connected by four $HMBI^-$ ligands (Fig. 1f). All Ni sites are four-coordinated and in the square-planar geometry. All $HMBI^-$ ligands provide one N atom of the imidazole-group and one S atom of the mercapto-group to coordinate to $Ni1^{II}$ and $Ni2^{II}$ ions, respectively, giving rise to the final structure. Neighboring clusters connect with each other by intercluster interactions and weak hydrogen bonds to form a 3D supramolecular architecture (Fig. S8†).

Complex **8** is a pentanuclear nickel cluster with trigonal bipyramid shape (Fig. 1g). All Ni sites are tetracoordinated. All $HMBI^-$ ligands offer one N atom of the imidazole-group to coordinate to equatorial Ni^{II} ion and one S atom of the mercapto-group to bridge one axial Ni^{II} ion and one equatorial Ni^{II} ion in η^1:η^2:μ_3-mode. The equatorial Ni1/Ni1A/Ni1B features a square-planar $[NiN_2S_2]$ geometry formed by the coordination of two N atoms from two $HMBI^-$ ligands and two S atoms from two $HMBI^-$ ligands. The axial Ni2/Ni2A exhibits a tetrahedral $[NiOS_3]$ geometry fulfilled by the coordination of one O atom from the terminal ligand CH_3O^- and three S atoms from three $HMBI^-$ ligands. The π···π stacking of adjacent clusters results in 1D chains (Fig. S9†), which are further connected to 3D supramolecular framework *via* interchain interactions and weak hydrogen bonds of neighboring chains (Fig. S10†).

PXRD analyses

To confirm the phase purities of complexes **1** and **6** before magnetic measurements, PXRD (powder X-ray diffraction) analyses were performed. As shown in Fig. S11 and S12 (ESI†), the agreement of the PXRD patterns of the as-synthesized bulk crystals and those simulated from the single-crystal structures of **1** and **6** indicated that the single crystal structures represent the structures of the samples.

Magnetic Studies

The solid state magnetic susceptibility of **1** and **6** was measured in the 2–300 K range at a field of 1000 Oe and the isothermal field-dependent magnetizations $M(H)$ at 2 K at fields up to 70 kOe (All measurements were carried out on crushed crystalline samples). As shown in Fig. 2, the $\chi_M T$ value of complex **1** at 300 K is 6.62 cm^3 K mol^{-1}, which is smaller than the spin-only values (g = 2.0) expected for 4 isolated high-spin d^7 ions (7.50 cm^3 K mol^{-1}), suggesting the obvious antiferromagnetic (AF) couplings between Co^{II} ions. As the temperature is lowered, $\chi_M T$ decreases gradually to 0.015 cm^3 K mol^{-1} at 2 K, which may be attributed to the AF coupling and spin-orbital coupling of tetrahedral Co^{II} ions (single-ion effect). The large negative Weiss constant, θ = −288.6 K, derived from the Curie–Weiss law (Fig. S13†), implies overall strong intracluster AF interactions, which was further confirmed by field-dependent magnetizations at 2 K as the curve displays a linear increasing trend along with an increasing field and final reaches 0.052 Nβ at 7 T far from saturation (Fig. S14†). The strong AF couplings of the neighbouring Co^{II} ions in **1** is mainly ascribed to the *syn,syn*-carboxylate and μ_4-O^{2-} bridges.

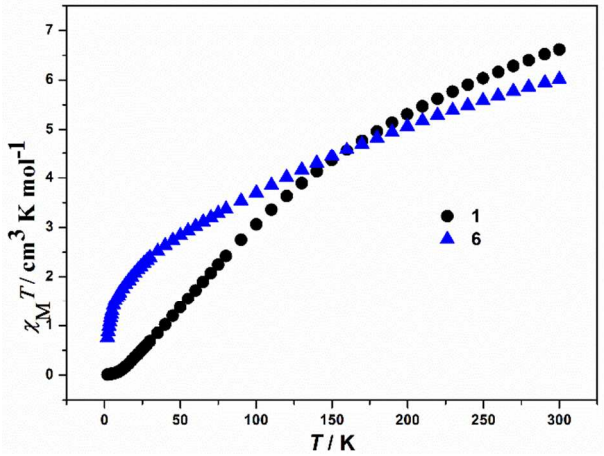

Fig. 2 Plot of $\chi_M T$ *vs* T for **1** and **6**.

The observed $\chi_M T$ products of 6.02 cm^3 K mol^{-1} at 300 K for **6** are smaller than the spin-only values (7.5 cm^3 K mol^{-1}, S = 3/2, g = 2.0) expected for four isolated high-spin d^7 ions, suggesting the presence of AF interaction. The AF coupling and spin-orbital coupling of tetrahedral Co^{II} ions (single-ion effect) are responsible for the monotonic decline of the $\chi_M T$ values of **6** with decreasing temperature. The large negative Weiss constant θ (-149.8 K) indicates global AF coupling in the molecular cluster (Fig. S15†), which is further confirmed by the M *vs.* H plot at 2 K: 2.06 Nβ at 7 T (Fig. S16†). It is notable that spin competition (frustration index, $f = |\theta|/T_N$ = 150/2 = 75) exists in **6** due to the triangular arrangement of the AF coupled Co^{II} ions in the cluster.

Conclusions

A series of cobalt and nickel clusters based on thiol-containing ligands (2-mercaptobenzothiazole and 2-mercaptobenzimidazole) accompanied by *in situ* ligand formation for 2-mercaptobenzothiazole have been reported. Magnetic measurements indicate that complexes **1** and **6** display AF behaviours. The result confirms the potential of generating novel molecular clusters through the sound choice of appropriate metal resource (precursors or metal salts) and thiol-containing ligands. The successful synthesis of **1-8** not only enriches the existing field of molecular clusters but also opens possibilities for synthesizing other novel polymetallic complexes via assembling different suitable metal resource and thiol-containing ligands.

Acknowledgements

We thank Dr. Tong-Liang Hu for very helpful discussion and suggestions. This work was supported by the 973 Program of China (Grant 2014CB845600), the NSF of China (Grants 21031002 and 21290171) and MOE Innovation Team (IRT13022) of China.

Notes and references

Department of Chemistry, TKL of Metal- and Molecule-Based Material Chemistry and Collaborative Innovation Center of Chemical Science and Engineering (Tianjin), Nankai University, Tianjin 300071, P.R. China.
E-mail: buxh@nankai.edu.cn. Fax: +86-22-23502458.
Electronic Supplementary Information (ESI) available: [crystallographic data in CIF or other electronic format see]. See DOI: 10.1039/c000000x/

1 (*a*) Z.-M. Zhang, Y.-G. Li, S. Yao, E.-B. Wang, Y.-H. Wang and R. Clérac, *Angew. Chem., Int. Ed.*, 2009, **48**, 1581; (*b*) S.-T. Zheng, T. Wu, B. Irfanoglu, F. Zuo, P. Feng and X. Bu, *Angew. Chem., Int. Ed.*, 2011, **50**, 8034; (*c*) H. Tan, S. Du, Y. Bi and W. Liao, *Chem. Commun.*, 2013, **49**, 8211; (*d*) P. King, T. C. Stamatatos, K. A. Abboud and G. Christou, *Angew. Chem., Int. Ed.*, 2006, **45**, 7379; (*e*) A. L. Dearden, S. Parsons and R. E. P. Winpenny, *Angew. Chem., Int. Ed.*, 2001, **40**, 151.

2 (*a*) Y. Bi, X.-T. Wang, W. Liao, X. Wang, X. Wang, H. Zhang and S. Gao, *J. Am. Chem. Soc.*, 2009, **131**, 11650; (*b*) C.-M. Liu, D.-Q. Zhang, X. Hao and D.-B. Zhu, *Chem.–Eur. J.*, 2011, **17**, 12285; (*c*) J. Li, J. Tao, R.-B. Huang and L.-S. Zheng, *Inorg. Chem.*, 2012, **51**, 5988; (*d*) C.-Z. Ruan, R. Wen, M.-X. Liang, X.-J. Kong, Y.-P. Ren, L.-S. Long, R.-B. Huang and L.-S. Zheng, *Inorg. Chem.*, 2012, **51**, 7587; (*e*) L. Lisnard, F. Tuna, A. Candini, M. Affronte, R. E. P. Winpenny and E. J. L. McInnes, *Angew. Chem., Int. Ed.*, 2008, **47**, 9695.

3 (*a*) C. E. Anson, A. Eichhöfer, I. Issac, D. Fenske, O. Fuhr, P. Sevillano, C. Persau, D. Stalke and J. Zhang, *Angew. Chem., Int. Ed.*, 2008, **47**, 1326; (*b*) A. Müller, E. Beckmann, H. Bögge, M. Schmidtmann and A. Dress, *Angew. Chem., Int. Ed.*, 2002, **41**, 1162; (*c*) A. J. Tasiopoulos, A. Vinslava, W. Wernsdorfer, K. A. Abboud and G. Christou, *Angew. Chem., Int. Ed.*, 2004, **43**, 2117; (*d*) Z.-M. Zhang, S. Yao, Y.-G. Li, R. Clérac, Y. Lu, Z.-M. Su and E.-B. Wang, *J. Am. Chem. Soc.*, 2009, **131**, 14600; (*e*) P. Alborés and E. Rentschler, *Angew. Chem., Int. Ed.*, 2009, **48**, 9366; (*f*) D. Fenske, J. Ohmer and J. Hachgenei, *Angew. Chem. Int. Ed. Engl.*, 1985, **24**, 993; (*g*) X.-J. Kong, Y.-L. Wu, L.-S. Long, L.-S. Zheng and Z.-P. Zheng, *J. Am. Chem. Soc.*, 2009, **131**, 6918; (*h*) X.-J. Kong, L.-S. Long, R.-B. Huang, L.-S. Zheng, T. D. Harrisc and Z.-P. Zheng, *Chem. Commun.* 2009, 4354; (*i*) W.-G. Wang, A.-J. Zhou, W.-X. Zhang, M.-L. Tong, X.-M. Chen, M. Nakano, C. C. Beedle and D. N. Hendrickson, *J. Am. Chem. Soc.*, 2007, **129**, 1014; (*j*) A. Baniodeh, I. J. Hewitt, V. Mereacre, Y.-H. Lan, G. Novitchi, C. E. Anson and A. K. Powell, *Dalton Trans.*, 2011, **40**, 4080.

4 (*a*) R. Sessoli, D. Gatteschi, A. Caneschi and M. A. Novak, *Nature* 1993, **365**, 141; (*b*) M. Manoli, R. Inglis, M. J. Manos, V. Nastopoulos, W. Wernsdorfer, E. K. Brechin and A. J. Tasiopoulos, *Angew. Chem., Int. Ed.*, 2011, **50**, 4441; (*c*) A. L. Barra, A. Caneschi, A. Cornia, F. F. De Biani, D. Gatteschi, C. Sangregorio, R. Sessoli and L. Sorace, *J. Am. Chem. Soc.*, 1999, **121**, 5302; (*d*) F. S. Guo, Y. C. Chen, L. L. Mao, W. Q. Lin, J. D. Leng, R. Tarasenko, M. Orendáč, J. Prokleška, V. Sechovský and M. L. Tong, *Chem.-Eur. J.,* 2013, **19**, 14876; (*e*) Y.-F. Zeng, G.-C. Xu, X. Hu, Z. Chen, X.-H. Bu, S. Gao and E. C. Sañudo, *Inorg. Chem.*, 2010, **49**, 9734; (*f*) X.-J. Kong, Y.-P. Ren, L.-S. Long, Z.-P. Zheng, R.-B. Huang and L.-S. Zheng, *J. Am. Chem. Soc.*, 2007, **129**, 7016; (*g*) J.-D. Leng, J.-L. Liu and M.-L. Tong, *Chem. Commun.*, 2012, **48**, 5286; (*h*) J.-B. Peng, Q.-C. Zhang, X.-J. Kong, Y.-P. Ren, L.-S. Long, R.-B. Huang, L.-S. Zheng and Z. Zheng, *Angew. Chem., Int. Ed.*, 2011, **50**, 10649.

5 (*a*) D. Foguet-Albiol, K. A. Abboud and G. Christou, *Chem. Commun.*, 2005, 4282; (*b*) A. Ferguson, A. Parkin, J. Sanchez-Benitez, K. Kamenev, W. Wernsdorferc and M. Murrie, *Chem. Commun.*, 2007, 3473; (*c*) Z.-G. Gu and S. C. Sevov, *Inorg. Chem.*, 2009, **48**, 8066; (*d*) R. E. P. Winpenny, *Adv. Inorg. Chem.*, 2001, **52**, 1; (*e*) R. W. Saalfrank, H. Maid and A. Scheurer, *Angew. Chem., Int. Ed.*, 2008, **47**, 8794.

6 (*a*) C. W. Liu, M. D. Irwin, A. A. Mohamed, J. P. Fackler Junior, *Inorg. Chim. Acta*, 2004, **357**, 3950; (*b*) J. Han and D. Coucouvanis, *Inorg. Chem.*, 2002, **41**, 2738; (*c*) S. A. Ivanov, M. A. Kozee, W. A. Merrill, S. Agarwal and L. F. Dahl, *J. Chem. Soc., Dalton Trans.*, 2002, 4105; (*d*) G. Han, D. Guo, C.-Y. Duan, H. Mo and Q. Meng, *New J. Chem.*, 2002, **26**, 1371; (*e*) J. J. Guo, W. Wang, Y.-D. Zhang, L. Yang, S.-H. Zhang and X.-Q. Zhang, *J. Coord. Chem.*, 2013, **66**, 1467; (*f*) F. Jian, H. Xiao, Z. Bai and P. Zhao, *J. Mater. Chem.*, 2006, **16**, 3746.

7 F. Tuna, C. A. Smith, M. Bodensteiner, L. Ungur, L. F. Chibotaru, E. J. L. McInnes, R. E. P. Winpenny, D. Collison and R. A. Layfield, *Angew. Chem., Int. Ed.*, 2012, **51**, 6976.

8 (*a*) S.-D. Han, Y.-Q. Chen, J.-P. Zhao, S.-J. Liu, X.-H. Miao, T.-L. Hu and X.-H. Bu, *CrystEngComm*, 2014, **16**, 753; (*b*) S.-D. Han, X.-H. Miao, S.-J. Liu and X.-H. Bu, *Inorg. Chem. Front.*, 2014, **1**, 549.

9 For examples, see: (*a*) S.-J. Liu, J.-P. Zhao, J. Tao, J.-M. Jia, S.-D. Han, Y. Li, Y.-C. Chen, and X.-H. Bu, *Inorg. Chem.*, 2013, **52**, 9163; (*b*) Y.-Q. Chen, G.-R. Li, Z. Chang, Y.-K. Qu, Y.-H. Zhang and X.-H. Bu, *Chem. Sci.*, 2013, **4**, 3678; (*c*) S.-D. Han, J.-P. Zhao, Y.-Q. Chen, S.-J. Liu, X.-H. Miao, T.-L. Hu, and X.-H. Bu, *Cryst. Growth Des.,* 2014, **14**, 2.

10 (*a*) G. Aromí, A. S. Batsanov, P. Christian, M. Helliwell, A. Parkin, S. Parsons, A. A. Smith, G. A. Timco and R. E. P. Winpenny, *Chem.–Eur. J.*, 2003, **9**, 5142; (*b*) E. Burzurí, J. Campo, L. R. Falvello, E. Forcén-Vázquez, F. Luis, I. Mayoral, F. Palacio, C. Sáenz de Pipaón and M. Tomás, *Chem.–Eur. J.*, 2011, **17**, 2818; (*c*) V. Mereacre, D. Prodius, Y. Lan, C. Turta, C. E. Anson and A. K. Powell, *Chem.–Eur. J.*, 2011, **17**, 123; (*d*) T. N. Nguyen, W. Wernsdorfer, K. A. Abboud and G. Christou, *J. Am. Chem. Soc.*, 2011, **133**, 20688; (*e*) A. J. Tasiopoulos, A. Vinslava, W. Wernsdorfer, K. A. Abboud and G. Christou, *Angew. Chem., Int. Ed.*, 2004, **43**, 2117; (*f*) S.-J. Liu, Y.-F. Zeng, L. Xue, S.-D. Han, J.-M. Jia, T.-L. Hu and X.-H. Bu, *Inorg. Chem. Front.*, 2014, **1**, 200; (*g*) Y.-Z. Zheng, M. Evangelisti and R. E. P. Winpenny, *Angew. Chem., Int. Ed.*, 2011, **50**, 3692; (*h*) Y.-L. Bai, J. Tao, W. Wernsdorfer, O. Sato, R.-B. Huang and L.-S. Zheng, *J. Am. Chem. Soc.*, 2006, **128**, 16428; (*i*) A.-L. Cheng, N. Liu, J.-Y. Zhang and E.-Q. Gao, *Inorg. Chem.*, 2007, **46**, 1034; (*j*) P. Alborés and E. Rentschler, *Dalton Trans.*, 2009, 2609; (*k*) S.-D. Han, W.-C. Song, J.-P. Zhao, Q. Yang, S.-J. Liu, Y. Li and X.-H. Bu, *Chem. Commun.*, 2013, **49**, 871.

11 G. Chaboussant, R. Basler, H.-U. Güdel, S. T. Ochsenbein, A. Parkin, S. Parsons, G. Rajaraman, A. Sieber, A. A. Smith, G. A. Timco and R. E. P. Winpenny, *Dalton Trans.*, 2004, 2758.

12 Rigaku, Process-Auto; Rigaku Americas Corporation: The Woodlands, Texas, 1998.

13 G. M. Sheldrick, *SHELXS97 Program for Solution of Crystal Structures*, University of Göttingen, Göttingen, Germany, 1997.

14 A. L. Spek, *J. Appl. Crystallogr.*, 2003, **36**, 7.
15 (a) J. Torres-Nieto, W. W. Brennessel, W. D. Jones and J. J. García, *J. Am. Chem. Soc.*, 2009, **131**, 4120; (*b*) D. A. Vicic and W. D. Jones, *J. Am. Chem. Soc.*, 1999, **121**, 7606.
16 X.-J. Kong, G.-L. Zhuang, Y.-P. Ren, L.-S. Long, R.-B. Huang and L.-S. Zheng, *Dalton Trans.*, 2009, 1707, and references cited therein.
17 M. E. Nikiforova, M. O. Talismanova, G. G. Aleksandrov, S. K. Kotovskaya, A. A. Sidorov, V. M. Novotortsev, V. N. Ikorskii, V. N. Charushin, I. L. Eremenko and I. I. Moiseev, *Russ. Chem. Bull.*, 2006, **55**, 2181.

Graphic Abstract

A Series of Cobalt and Nickel Clusters Based on Thiol-containing Ligands Accompanied by *in situ* Ligand Formation

Song-De Han, Xiao-Hong Miao, Sui-Jun Liu, Tong-Liang Hu and Xian-He Bu*

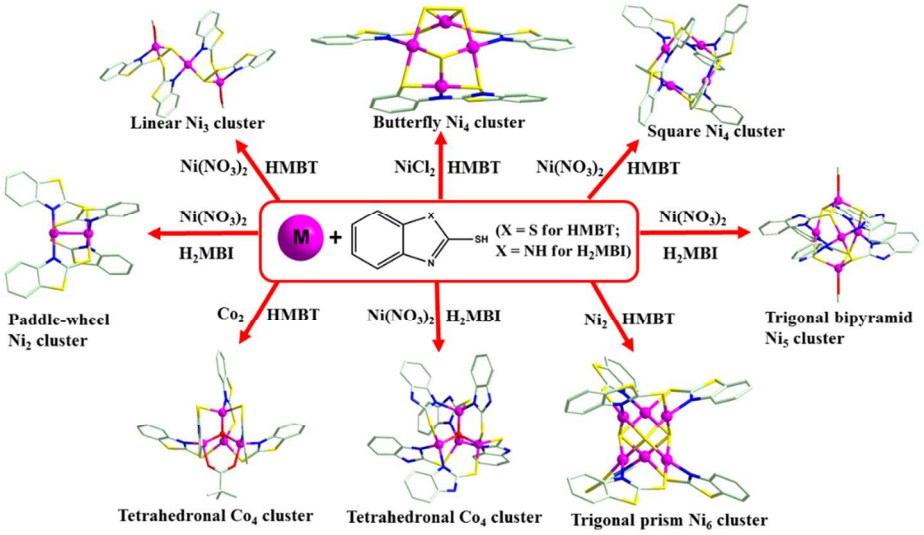

We report a series of cobalt and nickel clusters based on thiol-containing ligands, 2-mercaptobenzothiazole (HMBT) and 2-mercaptobenzimidazole (H_2MBI), accompanied by *in situ* ligand transformation for HMBT. Magnetic properties of the cobalt clusters have been investigated.